High-speed freight trains for intermodal transportation: Wind tunnel study on the aerodynamic coefficients of container wagons

S. Giappino, S. Melzi, G. Tomasini *

Department of Mechanical Engineering, Politecnico di Milano, Italy

The paper investigates the response to crosswind of a high-speed freight train for intermodal transportation, through wind tunnel tests. A 1:20 model of a freight train composed by an engine and two flat-car vehicles was instrumented with force balances to measure the aerodynamic coefficients of the flat-car plus container assembly and of the container alone. Aerodynamic coefficients strongly affects the train stability and the anchorage limits of the container itself.

During the wind tunnel tests, eight different loading configurations were considered and aerodynamic co-efficients were determined for yaw angles (i.e. angle between train and wind) ranging from 0° to 90°. Experi-mental results show the benefits in terms of drag reduction due to the presence of a laden vehicle upstream. As far as the rollover risk is concerned, the less critical condition is found for a vehicle preceded by a fully laden wagon and followed by an empty one. More in particular, at low yaw angles, the worst condition for a vehicle occurs when the wagon ahead is empty while, for yaw angles between 45° and 55°, which are the most critical for 'low speed' trains, the differences with respect to the other configurations reduce significantly.

Keywords: Intermodal freight train, Cross wind, Container, Aerodynamic coefficients, Drag, Aerodynamic efficiency

1. Introduction

The investigation of railway vehicles aerodynamics is of great importance both for economic and safety reasons; in fact, knowing the wind loads acting on a train-set allows, on the one hand, to address energy consumption issues and, on the other hand, to study the aerodynamic stability of the train. In this field, research has been mainly focused on passenger trains as they travel at higher speeds and are much lightweight with respect to freight trains (Baker et al., 2009; Baker, 2013; Cui et al., 2014; Dorigatti et al., 2015; Paradot et al., 2015; Premoli et al., 2016).

In recent years, environmental concerns and cost savings opportunities (at least for long-medium distances), increased the interest towards goods transportation by means of freight trains. However, simpler logistics management and door to door operation, still represent factors making road transportation strongly attractive. Increasing operating speed of freight trains appears as a way to improve the competitiveness of rail transportation overcoming part of its logistics limits.

In general, high speed poses a series of safety issues associated with the dynamics of the whole trainset and of the single vehicle (Cheli, Di Gialleonardo, Melzi). In the specific case of freight trains, due to the poor aerodynamic characteristics of the wagons, also crosswind may influence running stability even for speed below 200 km/h (Giappino et al., 2016). Moreover, intermodal freight trains carrying shipping containers, are characterised by wagons of various sizes, known as flatcars, well-cars and skeletonised cars. As a consequence, while in passenger trains wagons are in tight composition and the front section of a vehicle is not directly exposed to wind, in intermodal freight trains a significant gap between adjacent vehicles may be present. This variable loading configuration can have a strong impact on both the running safety, due to the overturning risk associated to cross wind but also the energy consumption and, thus, the transportation costs, especially when high-speed operation is required.

The necessity to operate goods trains at higher speed has thus given an impulse to the study of the aerodynamics of freight wagons with a particular focus on the optimization of the loading configuration of train used for intermodal transport.

Researches carried out in recent years are mainly focused on the analysis of aerodynamic efficiency, by using CFD analysis and wind tunnel tests. Considering the most recent ones, the evaluation of the aerodynamic drag coefficient with CFD analysis in Kedare et al. (2015) is performed for two different wagons geometries while in Östh and Krajnović (2014) allows to determine the effect of the boundary conditions. According to the study carried out by Östh and Krajnović, the drag

Received 26 October 2017;
Received in revised form 29 January 2018;
Accepted 30 January 2018

* Corresponding author.
E-mail address: gisella.tomasini@polimi.it (G. Tomasini).

coefficient of the wagon when included in the train was found to be 90% lower than a wagon in free-stream. More recently, the effect on the drag of the wagon length and position in a train was numerically studied in Maleki et al. (2017), also accounting for upstream and downstream gap spacings. This last work is based on wind tunnel tests carried out with the same scope on reduced-scale wagon models as described in Li et al. (2017).

In alternative to CFD and wind tunnel analyses, semi-empirical formulations were proposed to predict the drag on a single vehicle in a given position along a train-set and to estimate the overall drag of a train (Lai et al., 2008b; Beagles and Fletcher, 2013). Evaluation of the efficiency of a load configuration and methods for its optimization are presented in Lai et al. (2008a).

Effects of aerodynamics on running safety did not receive the same attention, though the importance of this investigation was also remarked by the evidence of some crosswind accidents, which involved empty containers being blown away by the wind (Rail Accident Investigation Branch (RAIB), 2008). In Alam and Watkins (2007a) and Alam and Watkins (2007b), wind tunnel tests with a specific container wagon (double stacked) are performed to evaluated the aerodynamic coefficients as a function of the wind angles: the main limitation of these results is that they refer to a wagon in isolation, without accounting for the presence of the other wagons. Hemida and Baker (Hemida and Baker, 2010) evaluate the aerodynamic coefficients of a generic container wagon (single-stacked) using large-eddy simulation and accounting for the influences of the neighbouring wagons by imposing spanwise periodicity. The results are obtained for a crosswind at 90° yaw angle, with and without moving ground simulation. In Zhou et al. (2007), CFD analysis is used to compare, in terms of aerodynamic coefficients, different types of wagons while in Li and Tian (2012), the effect on the overturning risk due to cross wind of specific cross-loading structures positioned in correspondence of the gap between wagons, is studied by means of wind tunnel tests for double-deck vehicles. A more general study on the effect of the container loading efficiency and the presence of gap in front or behind a container on the aerodynamic coefficients is carried out in Soper et al. (2015), by means of moving model cross wind experiments conducted at the University of Birmingham's TRAIN rig facility. The tests, carried out at a yaw angle of 30° for three different consists, allowed to conclude that a reduced loading efficiency and, in particular, the presence of a gap in front of the container lead to an increasing on the aerodynamic forces and, as a consequence, to an higher overturning risk.

In this work, a more general analysis of the aerodynamics of a freight train for intermodal transportation was experimentally carried out by means of wind tunnel tests on steady models. A 1:20 model of a trainset made up of three vehicles (1 engine and 2 flat car wagons) was analysed considering eight different loading configurations and measuring the forces and moments generated by relative wind.

The main goal of this work is to evaluate the effects of different loading configurations at different yaw angles on the rollover moment coefficient, in order to find the best configuration minimizing the overturning risk associated to the cross wind. In particular, with respect to the results already presented in technical literature, in this work aerodynamic coefficients were identified for all yaw angles between wind and train-set ranging from 0° to 90°. In fact, as demonstrated in Giappino et al. (2016), due to the low operating speed, the range of critical yaw angle for lightweight railway vehicles for urban and suburban use, is between 40° and 55°. Critical yaw angles for high-speed trains are instead between 10° and 30°.

Moreover, the Characteristic Wind Curves of low-speed trains are generally more sensible to the wind direction than that of high-speed trains; for these reasons, in order to correctly evaluate the overturning risk of such a vehicles, it is important to analyse the whole distribution of the coefficients over the angles of attack. In addition, considering that the lateral wind is critical not only for the overturning risk but also for the anchorage of the container itself, the aerodynamic coefficients have been evaluated on both the whole of wagon (flat-car + container) and the only container. Finally, focusing the analysis on the drag coefficient with lateral wind, the effect of different configurations on the aerodynamic efficiency was evaluated.

In the next section the experimental wind tunnel setup and the tested configurations are described while in section 3 the results are shown and discussed.

The research activity presented in this paper is part of SIFEG project funded by the Italian Ministry of Economic Development (MISE). The project aims at increasing competitiveness of rail transportation by improving its logistic aspects and by designing high-speed container trains able to operate on high speed lines.

2. Wind tunnel tests

2.1. Test characteristics

Wind tunnel tests were performed on a 1:20 scale model of a freight train (Fig. 1). The convoy was tested in a flat-ground scenario (without ballast and rails), which is one of the reference scenarios described in the TSI 232/2008 standard European Rail Agency (2008).

The train model is composed by 3 vehicles: one front engine and two freight carriages instrumented to measure the aerodynamic forces.

The convoy composition was chosen in order on the basis of a trade-off between the minimum Re number required by the EN 14067-6 ($Re = 2.5\,10^5$) and the minimum number of vehicles necessary to correctly account for the boundary conditions to evaluate the crosswind performance of a railway vehicle (Baker et al., 2009; Baker, 2013). The selected solution complies with the requirements of the international standards (TSI 232/2008 and EN 14067-6) for the evaluation of the aerodynamic coefficients useful for the crosswind analysis, which is the main objective of the present paper. On the other hand, the authors are aware that the low number of vehicles penalises the correct evaluation of the drag coefficient, especially in terms of absolute value. In Golovanevskiy et al. (2012), the authors state, by means of numerical and wind tunnel experimental tests, that for long open cargo railway trains the model consisting of six rail cars with two streamlined bodies is the optimal configuration. Otherwise, from the presented results, it is possible to see that the main effects, due to different long compositions, are on the drag coefficient values and that the trend of this coefficient with the angle of attack is not influenced by the number of vehicles in the composition.

The wind tunnel is a closed circuit facility in vertical arrangement having two test sections, a 4×4 m^2 high speed low turbulence and a 14×4 m^2 low speed boundary layer test section. Tests were carried out in the High-Speed test section, whose characteristics are listed in Table 1. The test chamber is provided with a turntable (diameter 2.5 m) allowing to vary the yaw angle.

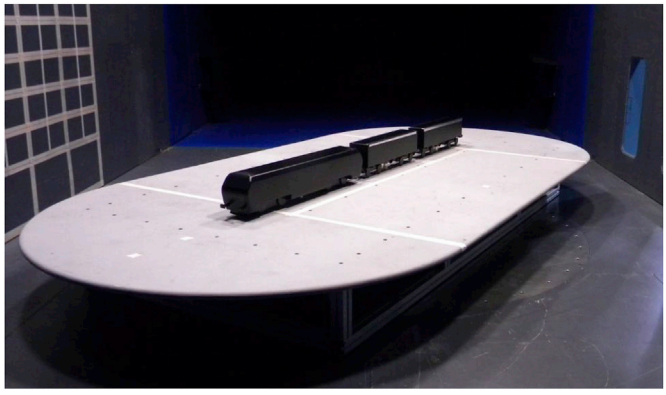

Fig. 1. 1:20 scaled model of the convoy in the High-Speed test section of the Politecnico di Milano Wind Tunnel.

Table 1
Main characteristics of the high-speed test section.

Size	Maximum speed	ΔU/U	I_t
4 × 4	55 m/s	< ±0.2%	<0.1%

Tests were performed in the high-speed test section in conditions of low turbulence, with different Reynolds numbers, in agreement with the requirements of TSI 232/2008 ($Tu_x \leq 2.5\%$, par. G.5.1.2.2, European Rail Agency (2008)).

2.1.1. Flow characteristics

The turbulence level of the test section is equal to 0.1%; this value is lower than the maximum one allowed by TSI 232/2008 European Rail Agency (2008). The model is set over a splitter plate to correctly reproduce the block profile required by the standard,. The dimensions of the plate are 2.5 m × 3.8 m. The corresponding boundary layer thickness at model location on the ground board, δ95%, is approximately 61 mm (about 45 mm from the top of the rail) corresponding to nearly 22% the vehicle height in agreement with the TSI European Rail Agency (2008), G.5.1.2.3.

The wind tunnel tests in the high-speed test section were performed with different wind speeds ranged between $U = 10$ m/s and $U = 50$ m/s. The corresponding Reynolds numbers, computed with the characteristic dimension h equal to the reference height ($h = 3$ m at real scale) range from $1{\cdot}10^5$ to $5{\cdot}10^5$.

According to the TSI 232/2008 (par. G 5.1.2.4 European Rail Agency (2008)), the Reynolds number independency is investigated in the range $0.2\ Re_{max} \div Re_{max}$.

The maximum blockage ratio B has to be defined at a yaw angle of 30° (par. G 5.1.2.1, European Rail Agency (2008)). It is calculated as the ratio of the total modelled configuration (train model + flat ground) projected side area to the wind tunnel cross section. For the considered configuration, this parameter is equal to 4.85%. In agreement with the requirements of European Rail Agency (2008), the blockage ratio is smaller than 10%. According to the normative, for closed test section with this value of blockage ratio no blockage correction is needed.

As required in the TSI 232/2008, tests are performed in low turbulence and steady-state conditions even if these ones may differ from the real ones. Actually, according to numerical and experimental analyses on different trains (Premoli et al., 2016, Hemida and Baker, 2010, Zhang et al., 2016, Cheli et al., 2013, Niu et al., 2017), the aerodynamic coefficients in real operating conditions (with moving models and turbulence) may differ from the ones measured in these simplified tests by 5%–15%. However, wind tunnel tests performed in this research aimed at evaluating the effects of train-set composition, (especially of the gap between containers) on aerodynamic coefficients. These effects are associated to macro physical mechanisms affecting the separation size and the nature of boundary layer enveloping the wagon (Li et al., 2017) and are not significantly influenced by the atmospheric boundary layer and not steady-state conditions (Hemida and Baker, 2010, Soper et al., 2015). In conclusion, considering the target of the analysis and the expected effect of atmospheric boundary layer and moving ground, the adopted experimental set-up was considered adequate for the purpose.

2.2. Train-set model

As already mentioned, the trainset tested in the wind tunnel is made up of one front engine and two wagons.

Table 2 lists the three main dimensions, length, width and height of the full scale vehicles and the nominal dimensions for the 1:20 scaled model.

The focus of the research consists on measuring the global aerodynamic forces and moments acting on each wagon and on each container individually. Therefore, particular care was taken when designing the model of the wagons, so that miniaturized force balances could be secured on the flat car allowing measurement of aerodynamic forces and moments on the container.

Table 2
Overall dimensions of the real vehicles and corresponding models.

	Real values [mm]	1/20 scale nominal values [mm]
Engine length	18480	924
Engine width	2920	146
Engine height	3620	181
Wagon length	12800	640
Wagon width	2438	121.9
Wagon height	3792	189.6

The models of the engine and the containers were built with machine-cut polyurethane model boards, while the flat-car are made of aluminium. Each vehicle is equipped with a steel pole (Fig. 2) providing the constraint to the scenario; as far as the wagons is concerned, the steel poles are linked to two 6-components force balances; the engine is instead directly fasten on the scenario. The stiffness of the fastening system is high enough to ensure that the dynamics of the model is negligible. The constraints allow to adjust the position of the three vehicles along both longitudinal and vertical direction.

Fig. 3 shows the three vehicles, with particular focus on the model of a wagon; as can be noticed, the container can be easily linked to the balance fixed on the flat car.

2.2.1. Aerodynamic forces measurement

Two 6-components industrial RUAG model 192 force balances have been connected below the two freight carriages of the convoy to measure the global aerodynamic forces acting on the vehicles. The force balance is connected to the train model by means of a steel pole (Fig. 2) in the center of the underbody. The stiffness of the connection ensures that the aerodynamic forces that arise on all the external surfaces of the vehicle model are transferred only to the dynamometric balance.

The accuracy of the force measurements has been evaluated performing symmetry checks between positive and negative yaw angles coefficients: this method takes into account the uncertainties due to the instrument but also to the set-up layout. The value, expressed in terms of standard deviation of the corresponding force/moment coefficients is reported in Table 3.

A miniaturized six-components force balance (ATI model mini45) is located at the interface between each container and the flat car (Figs. 2 and 3); this allows to measure all the aerodynamic forces and moments exerted on the container alone. Each flat car is designed so that balances can be moved and fasten in three positions: a single balance at the center of a 40 ft container and two balances at the center of 2 20 ft containers. As shown in Fig. 2, models of the containers are provided with inner room designed to host the balance.

2.2.2. Aerodynamic force coefficients

According to the CEN standard (CEN, 2010), the non-dimensional coefficients are defined as follows:

$$C_{F_i} = \frac{F_i}{1/2\rho S\overline{U}^2} \qquad C_{M_i} = \frac{M_i}{1/2\rho hS\overline{U}^2} \tag{1}$$

where F_i (i = x,y,z) are the aerodynamic force components in the train's reference system (Fig. 4) and M_i (i = x,y,z) are the corresponding moments. In equation (1), ρ is the air density, $\overline{U}^2$ is the mean square value of the wind speed, h is equal to 3 m (full scale), and S is a standard reference surface equal to 10 m^2 (full scale). The components of forces and moments are expressed according to the CEN convention reported in Fig. 4.

All the coefficients are evaluated at the midpoint of the track at top of the rail (see Fig. 2), while the rolling moment is calculated both with

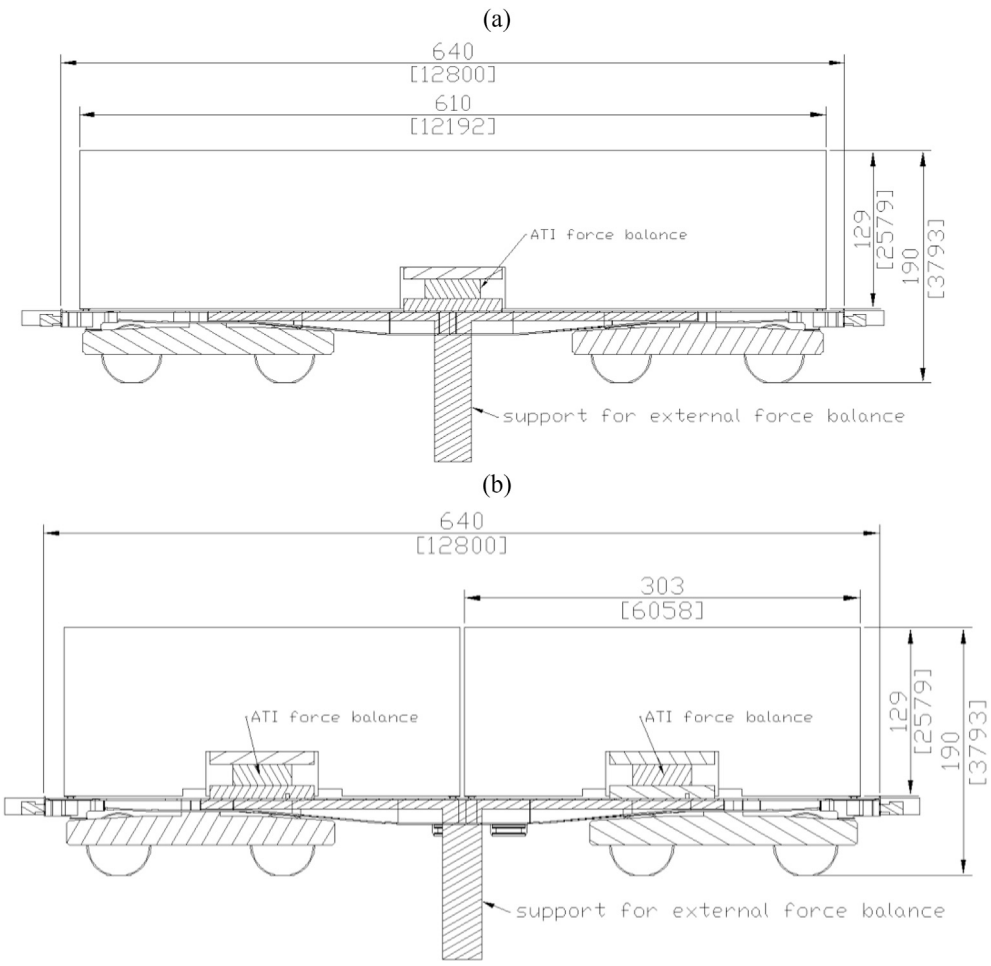

Fig. 2. Connections of the miniaturized internal force balance for the model of 40 ft container (12.19 m long) (a) and for the two models of 20 ft containers (6.1 m long). Dimensions in model scale and [full scale] milliliters.

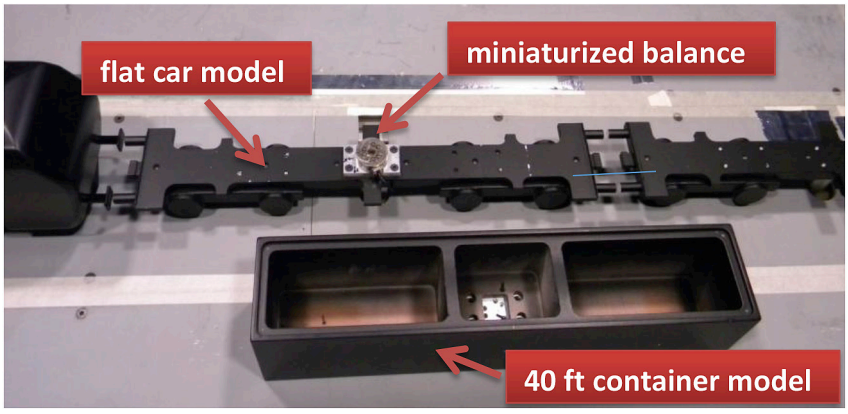

Fig. 3. Assembly of the experimental set up.

Table 3
Overall uncertainties associated to the dynamometric balance and to the whole experimental setup.

	C_{Fx}	C_{Fy}	C_{Fz}	$C_{Mx,lee}$
Vehicle	0.05	0.15	0.1	0.1
Container	–	–	0.13	0.05

respect to the middle of the track (CMx) and with respect to the lee rail (CMx lee).

In this study the same normalization was also used to calculate the force and moment coefficients on the containers alone. The use of a fixed reference area is helpful since the comparison of the force coefficients in different layouts means exactly a comparison in terms of wind force (all the wind forces have been normalized with the same area).

2.3. *Test conditions*

2.3.1. *Test scenario*

The infrastructure scenario is the flat ground one (TSI European Rail Agency (2008)). It was reproduced with a ground board in order to have a block profile of the mean wind speed (see Par. 2.1). The ground board is

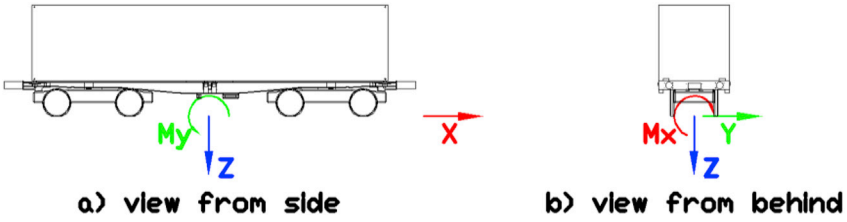

Fig. 4. Reference adopted for measuring forces and moments (CEN convention).

supported by an aluminium platform and the top is placed at a height of 0.350 m from the wind tunnel floor. Fig. 5 shows the configuration of testing within the walls of the high-speed test section.

2.3.2. Trainset layout

During the experimental campaign eight load layouts were tested, varying the size and the position of the gaps between the containers on the wagons, ranging from an unloaded condition to a full-load one (see Table 4). Two types of containers were considered:

- 40 ft container, 12.19 m long;
- 20 ft container, 6.1 m long.

3. Experimental results

Lateral wind loads are important both for the train stability but also for the anchorage of the container itself. The two topics are investigated separately in the two following paragraphs: section 3.1 refers to the overall wind load and the aerodynamic drag coefficient is also presented while section 3.2 refer to the container wind load.

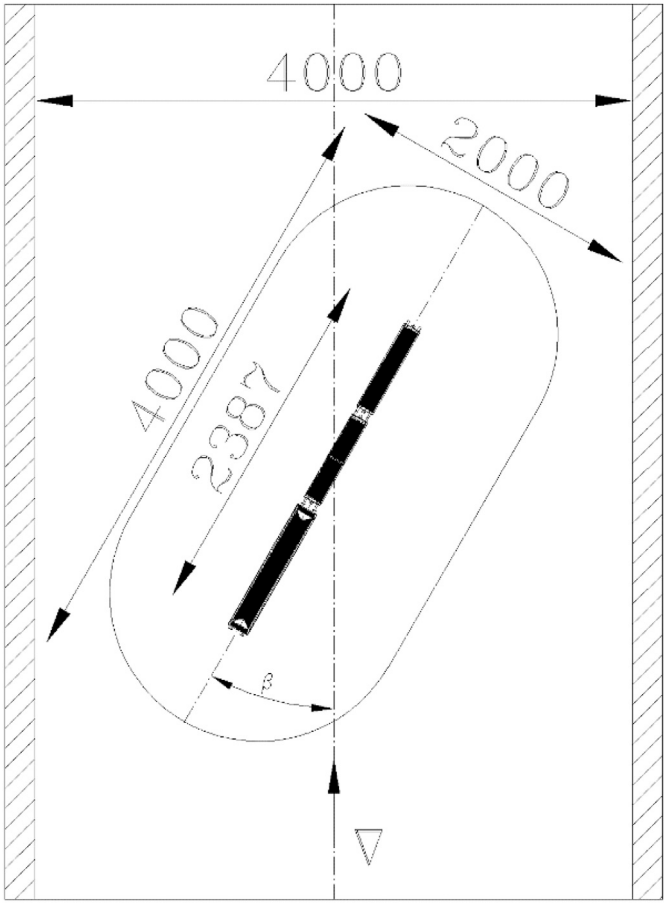

Fig. 5. Drawing of the scenario within the high speed test room.

Table 4
Trainset load distribution layouts.

Layout	1st wagon	2nd wagon	Scheme
1	40 ft container	40 ft container	2 1
2	40 ft container	1 20 ft container rear	2 1
3	40 ft container	2 20 ft containers	2 1
4	empty	2 20 ft containers	2 1
5	empty	1 20 ft container rear	2 1
6	empty	40 ft container	2 1
7	40 ft container	empty	2 1
8	empty	empty	2 1

3.1. Overall wind loads on wagons (flat-car + container)

We firstly investigate the trainset aerodynamic properties in terms of drag resistance: only the layouts with the 40 ft containers are included in the comparison, while the effect of the 20 ft containers are discussed in the following section. Fig. 6 shows the drag coefficient for the front (F) and rear (R) wagon in the different layouts. Results at yaw angle 0° are indicative for a train that is running without lateral wind: we identify the worst aerodynamic condition for the rear wagon of the layout L6 that is a wagon preceded by an empty one ($C_{Fx} = -0.55$). We measured the lower drag in the layout L1-F that is a wagon preceded by the power car and followed by another loaded wagon. Since the power car size is similar to the one of a loaded wagon, this layout can be also assumed as a container preceded and followed by a loaded one. The other intermediate conditions (L2-F, L7-F and L1-R) are representative of a wagon preceded by a loaded one and followed by an empty one. Also in this case the drag is higher than that found for the layout L1-F but the effect of a gap behind a wagon is lower than a gap in front the container. For comparison

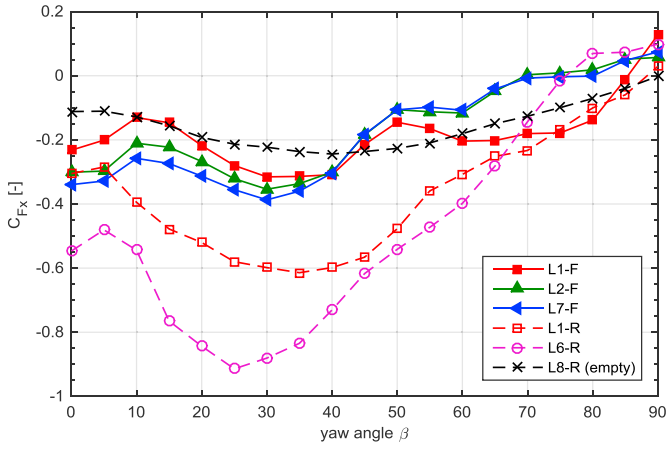

Fig. 6. Drag coefficient on the front (F) and rear (R) wagons for different trainset layouts.

purposes the drag for an empty vehicle (L8-R) is also presented in the graph. We can summarize that the presence of a loaded wagon in both positions (preceding and following) has a positive effect on the drag.

Similar qualitative conclusions can be found in Li et al. (2017), where the effects of gaps before and behind containers on aerodynamic drag are studied by means of wind tunnel tests on double-stacked containers. The authors point out that the front gap dominates the drag variation; moreover, experimental results reveal that drag is expected to increase when the front/rear gap is enlarged up to 12 times the width of the container. The only comparison we can perform to understand if different gaps lead to different drag variations, is between layout L1-R, characterized by an infinite rear gap (it is the last vehicle in the convoy), and layout L2-F, characterized by a rear gap of about 3 times the width of a container. At zero wind angle, the drag of these two configurations is almost the same; this result could be due mainly to the measurement uncertainty associated to the longitudinal component.

The presence of lateral wind has different effects on the longitudinal force coefficient: the layout L6-R has an almost constant drag up to 10° but for higher angles it strongly increases up to values higher (in magnitude) than $C_{Fx} = -0.9$. In the layout L1-F we observe a drag reduction in presence of small lateral winds ($\beta = 10deg$), but also in this case the drag than increases having a maximum at $\beta = 30deg$. The last vehicle of the convoy (L1-R) is strongly penalized by the lateral wind having the drag that is doubled at $\beta = 30deg$ with respect to 0.

In a similar way all the trainsets investigated shows the higher drag resistance at $\beta = 30deg$.

To investigate the crosswind effects, the most important forces are the moment coefficient with respect to the longitudinal axis C_{Mx}, the lateral force coefficient C_{Fy} (Fig. 7) and the vertical force coefficient C_{Fz} (Fig. 8). The combined effect of these forces in terms of rollover risk is often represented by the rolling moment coefficient with respect to the leeward rail $C_{Mx,lee}$ (Fig. 9), that is also used in the simplified method for the evaluation of the rollover risk in the European standard EN 14067-6 (CEN, 2010). The analysis is again limited to the 40 ft container trainsets. As observed in several studies, different behaviours are displayed as a function of yaw angles for front and rear vehicles. The first wagons show a monotonic increasing trend, up to about 50° followed by a decreasing one. The rear vehicles are instead characterized by an almost increasing trend up to 90° with a steeper gradient in the range 0°–45°.

A comparison in terms of values of aerodynamic coefficients can be made with Hemida and Baker, (2010) and Soper et al. (2015). In the first paper, CFD calculations were carried out on a freight train with several identical wagons at with crosswind at 90°. Computation resulted in coefficients almost double with respect to the values presented in this paper, but the wagon geometry and the boundary conditions are significantly different.

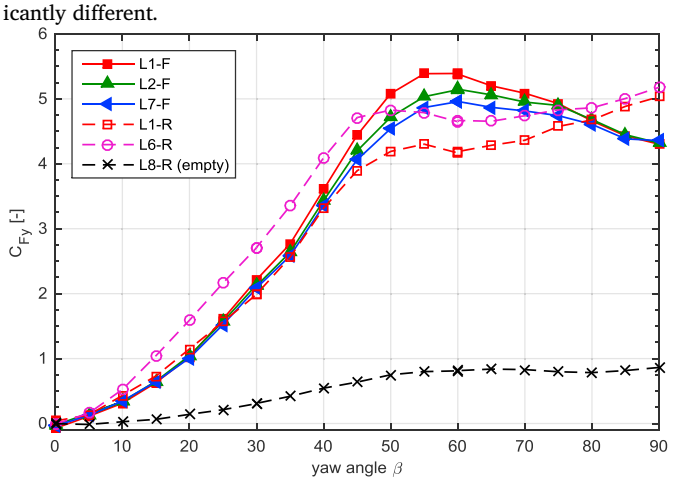

Fig. 7. Lateral force coefficient on the front (F) and rear (R) wagons for different trainset layouts.

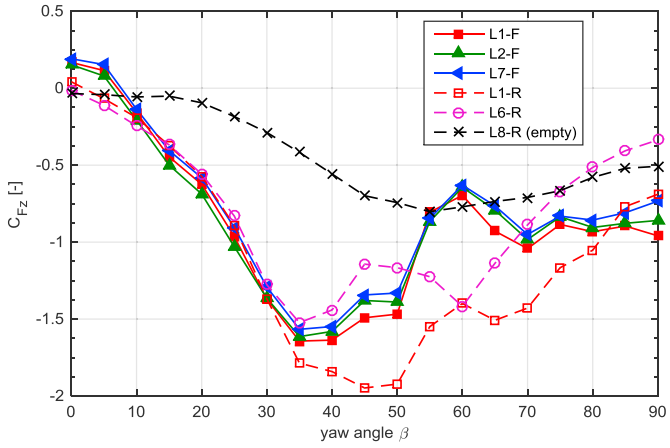

Fig. 8. Vertical force coefficient on the front (F) and rear (R) wagons for different trainset layouts.

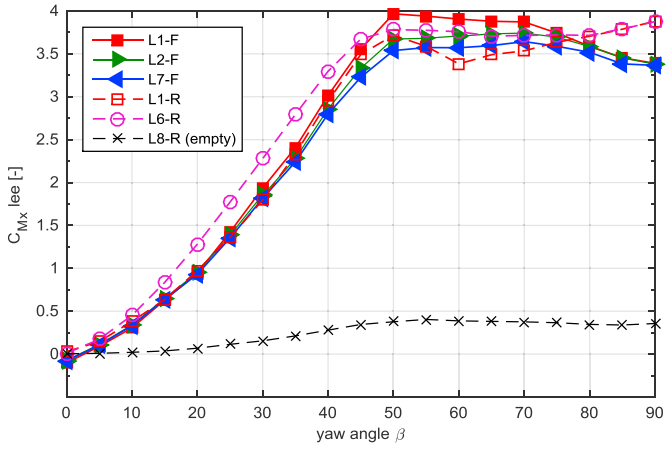

Fig. 9. Lee rail rolling moment coefficient on the front (F) and rear (R) wagons for different trainset layouts.

The moving-model tests with crosswind at 30° presented in Soper et al. (2015) allow to measure values closer to those of Figs. 7–9. For the configuration corresponding to the layout L1-F, the measured coefficients are $C_{Fy} = 1.7$ and $C_{Mx,lee} = 1.52$ (recalculated according to the coefficient definition adopted in this paper). Considering that the lateral area of the containers in Soper et al. (2015) is about 25% greater (container length L = 18.29 m), these coefficients rescaled are lower than the corresponding coefficients evaluated in this study of about 30%. Differences in terms of the absolute values can be justified considering that, in Soper et al. (2015), the model is moving and the forces are evaluated by discrete integration of the pressure distributions. The coefficient $C_{Fz} = 2.32$ is on the contrary higher than that plotted in Fig. 8 of about 20% but it is evaluated considering only the pressure distribution on the top of container and this leads, according to the same authors, to an overestimation of this value.

By observing Fig. 9, the worst absolute condition is visible for the layout L1-Front at 50° where $C_{Mx,lee}$ is close to 4. At smaller angles (<50°), the forces on a wagon that is preceded by an empty one (L6-R) can be up to 20% higher than in case of a fully loaded train (L1-F). Moreover, we can identify a small reduction effect at intermediate angles (30–50°) in the trainsets L2-F and L7-F that is caused by the following empty gap. The gap probably allows for a pressure recovery in the container downwind side reducing the suction.

At higher yaw angles (50°–60°), the worst condition for the crosswind risk is represented by the fully loaded train (L1-F) but, considering only the rear position in the convoy, the isolated wagon (configuration L6-R)

is more critical than the wagon preceded by a wagon and followed by an empty gap (L1-R) at all yaw angles.

It is possible to conclude that, for rear vehicles, the pejorative effect associated to a gap in front of the container reduces with increasing yaw angle and, for 'low-speed' trains, which are characterized by most critical angles between 40° and 55° (Giappino et al., 2016), this effect reduces to about 10%.

3.2. Wind loads on containers

In Fig. 10 a comparison between the lee-rail rolling moment coefficient measured on the 40 ft containers is presented. Since the major contribution to the lee-rail rolling moment is due to the lateral force, and this force is mainly associated to the wind action on the container and not on the flat car, conclusions similar to those drawn from the previous analysis can be found. In particular, Fig. 10 shows a comparison between the containers set respectively in the front position (first wagon, just after the locomotive, Fig. 10-a) and in the rear position (Fig. 10-b). In the first condition, as expected, the coefficients of layouts L1 and L3 are equivalent and greater than those of L2 and L7: indeed, in these last layouts, the container is followed by an empty wagon which allows a reduction of the suction on the container downwind surface and, as a consequence, a lower rolling moment. In Fig. 10-b, considering just the rear containers, as already observed in the analysis of the wagons, the presence of an empty flat wagon in front of a container increases the crosswind action and the lee-rail rolling moment of L6 is higher than that of L1; anyway, just around the most critical angles for 'low speed' trains (40°–55°), the difference between the two configurations reduces significantly. The intersection of the two curves at 40° is mainly is due to the vertical force coefficient (as shown in Giappino et al. (2014)) that reaches a higher value with the L1 configuration.

Finally, from the same figure and considering the L1-front and the L6-rear, it is possible to make a comparison between the two intermediate conditions, container preceded and followed by an empty wagon (L6) and container preceded and followed by fully loaded wagons (L1, front position). As found for the wagons, at low wind angles, L6 shows higher coefficients than L1 and then, for greater wind angles, the two curves are almost equivalent.

Fig. 11 shows the force coefficients on the small container (20 ft). Of course, due to the lateral surface that is halved, the overall forces are significantly lower than the ones on the 40 ft container. The lowest lee-rail rolling moment coefficients are those of L3 and L4 in rear position because they have in front of them a fully loaded wagon and behind an empty wagon: as already observed, both these conditions reduce the overturning coefficient and so these layouts represent the best configuration for the cross wind problem at all yaw angles. At 30° of yaw angle, the rolling moment coefficient of the layout L3-R is lower than the reference layout L3-F of about 26%. The layout L4-F is characterized by a container preceded by an empty wagon and followed by a fully loaded one; according to the findings already presented for the wagon and the 40 ft containers, this corresponds to the worst configuration. At a yaw angle of 30°, the rolling moment coefficient of L4-F is higher than the reference layout L3-F of about 37%. But, at higher yaw angles, and, in particular, in the range 40°–55°, the differences between these two configurations reduce significantly.

The other three layouts are characterized by intermediate conditions: in L2 and L5, containers are both preceded and followed by empty wagons; in L3-FRONT containers are preceded and followed by fully loaded wagons. As found for the 40 ft containers, at low wind angles, the worst operating condition is the one of L5 and L2 (with L2 a bit better, due to the shorter empty wagon in front of the container). On the other hand, at greater wind angles, the coefficient of layout L3-FRONT reaches the maximum and then remains significantly higher, to a constant value equivalent to that found with L4-FRONT. As shown in Fig. 12, this behavior is not associated to the rolling moment component, which is almost the same for the three layouts at angles higher than 60°, but is due

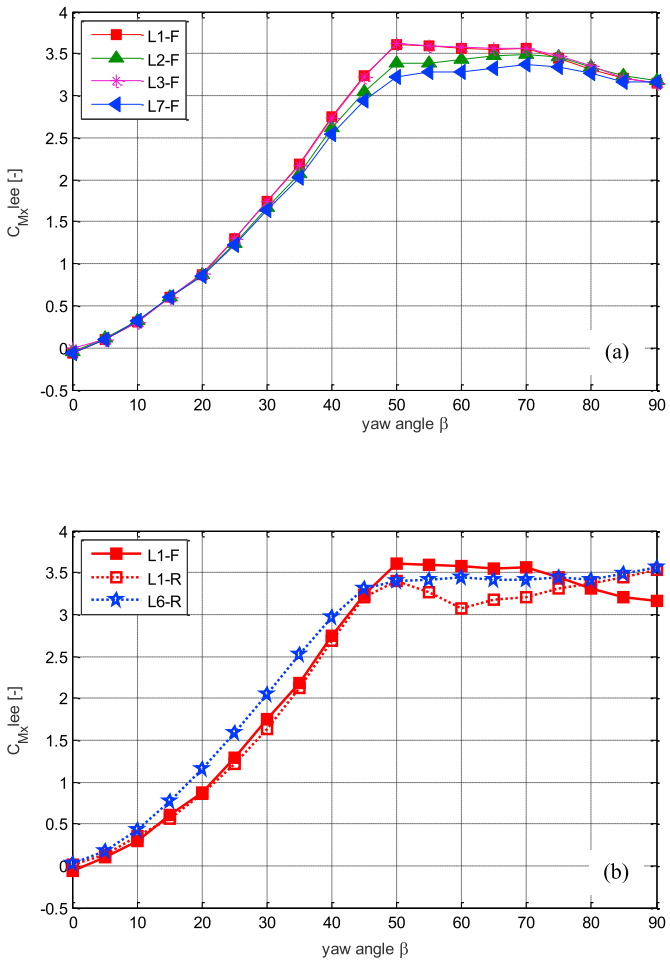

Fig. 10. Lee-rail rolling moment coefficients on the 40 ft container, comparison between the layouts: front position (a), rear position vs L1-front (b).

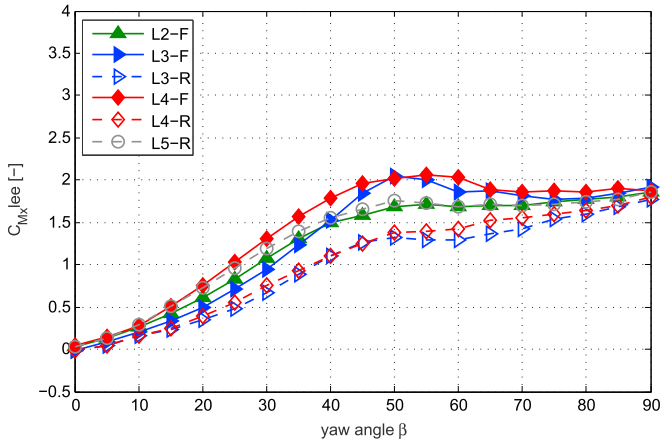

Fig. 11. Lee-rail rolling moment coefficients on the 20 ft container, comparison between the layouts.

to the vertical force coefficient. In the same range of wind angles, this coefficient with L3-FRONT layout reaches values 4 times higher than those measured with the other two considered layouts.

3.3. Discussion of the results

The analysis of the lee-rail rolling moment coefficient measured on the containers alone allows to confirm the results found for the whole

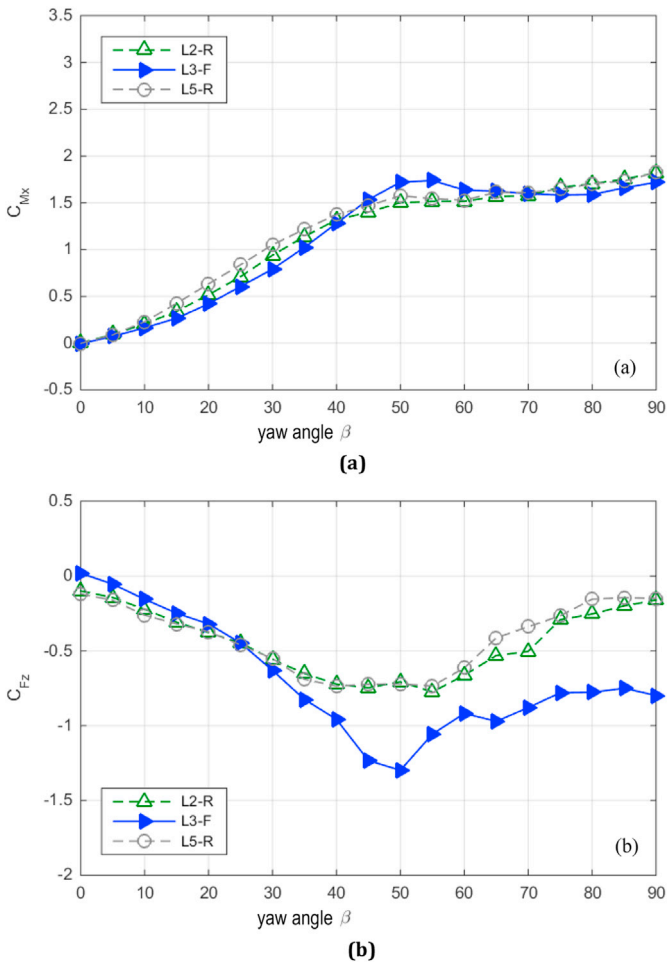

Fig. 12. Rolling moment coefficient (a) and vertical force coefficient (b) on the 20 ft container: comparison between the layouts L2-REAR, L3-FRONT and L5-REAR.

wagon also in the more variety of configurations tested with the 20 ft containers.

A similar analysis has been performed in Soper et al. (2015), by means of crosswind experiments on a moving-model of a freight train. Considering a 30° crosswind angle, the authors have compared a train with full loading efficiency with two reduced loading configuration trains. They have found that, with respect to the full loading configuration (equivalent to L1-F of this paper):

- a large gap before the measuring wagon leads to lateral force and rolling moment coefficients 25–30% higher, in agreement with the results presented in this paper, at the same yaw angle;
- a gap behind the measuring wagon leads to equivalent lateral forces but higher rolling moment, contrary to what observed in this paper.

In general, also considering the results of this paper, the effect associated to a gap in front of a container is quantitatively more significant than the effect of a gap in the rear.

Considering now the second comparison, as the lateral force is the same, we can conclude that the differences in the rolling moment are associated to the vertical force. As already mentioned, neglecting the pressure distribution in the underbody of the container could lead to uncertainties in the evaluation of vertical force and, consequently, in the rolling moment calculation. Finally, part of the differences observed in the second comparison, can also be due to a different gap behind the container.

In conclusion, the experimental results presented in this paper allowed to analyse how the differences between the layouts determined by the wind yaw angle. More in particular, the attention has been focused on the range of the critical angles of attack which, for freight trains with a maximum speed of $V_{max} = 120$ km/h, is higher than that typical for high speed trains ($V_{max} = 300$–350 km/h).

It has been found that, especially around these critical angles, the differences between the layouts at 30° are reduced and the lee-rail rolling moment is significantly influenced by the vertical force. On the other hand, this component is the most sensitive to the train-rail relative motion (Premoli et al., 2016), not reproduced with steady model tests, but very difficult to measure also with moving model tests (Soper et al., 2015).

For the future, more in-depth analyses, numerical or experimental, would be necessary to correctly measure this specific component in the interesting range of wind angles, accounting for the vehicle motion.

Finally, especially for the correct evaluation of the drag coefficient in terms of absolute value in presence of lateral wind, a convoy more complete and long should be useful.

4. Conclusions

The paper investigated the aerodynamic loads on freight trains by means of wind tunnel tests on reduced steady scaled models. Tests in this work have been carried out for all yaw angles between wind and train-set ranging from 0° to 90°, in order to correctly evaluate the risk of overturning accounting for all the possible directions of the relative wind-train velocity and, specifically, for the range of angles 40°–55°, which corresponds to the critical angles for 'low speed' trains ($V_{max} = 80$–120 km/h).

Analyses have been carried out for different layouts on lee-rail rolling moment coefficient, for the risks connected to the overturning due to crosswind and on longitudinal force coefficient, for the problems associated to the energy consumption. As expected, significant differences has been found depending on the pattern of the containers. As far as the longitudinal coefficient is concerned, the positive effects due to the presence of an upwind loaded vehicle are confirmed but also the presence of a following loaded vehicle gives additional benefits. Considering the lateral wind, we found some reduction at small yaw angles (10°) but at higher angles the drag always increases.

With regard to the lee rail rolling moment coefficient, by analysing both the whole wagons and the containers alone in a great variety of layouts, it is possible to conclude that, for the overturning risk and for the forces acting on the container anchorage:

- the better boundary condition for a wagon is to be preceded by a fully loaded wagon and followed by an empty wagon;
- for yaw angles up to 40°, the condition with a fully loaded wagon in the front and back is better than that with an empty wagon in the front and back (and, even more so, than that with an empty wagon just in the front, which represents the worse configuration). For angles between 45° and 55°, which are the most critical for 'low speed' trains, these differences reduce significantly and, in some cases, reverse.

The measured coefficients can be used by dynamic numerical multibody models which allow to calculate the Characteristic Wind Curves that are the limit wind speeds which make the vehicle overcome the rollover safety limits (TSI HS RST, 2008 and EN 14067-6, 2010). On the other hand, these curves are strictly related to the lee rail rolling moment coefficient and, consequently, a more general conclusion can be drawn right away. For the rollover risk to crosswind, in case of a freight convoy not fully loaded, it is safer to group all the containers in a way that they are adjacent each other rather than positioning each container isolated from the others.

Acknowledgements

The research activity presented in this paper, is part of SIFEG project funded by the Italian Ministry of Economic Development (MISE) (DM 00013MS01).

Appendix A. Supplementary data

Supplementary data related to this article can be found at https://doi.org/10.1016/j.jweia.2018.01.047.

References

Alam, F., Watkins, S., 2007. Effects of crosswinds on double stacked container wagons. In: Proceedings of the 16th Australasian Fluid Mechanics Conference, pp. 758–761, 16AFMC.

Alam, F., Watkins, S., December 2007. Lateral stability of a double stacked container wagon under crosswinds. In: The International Conference on Mechanical Engineering, Dhaka, Bangladesh, 29–31, pp. 79–85.

Baker, C.J., 2013. A framework for the consideration of the effects of crosswinds on trains. J. Wind Eng. Ind. Aerod. 123, 130–142.

Baker, C., Cheli, F., Orellano, A., Paradot, N., Proppe, C., Rocchi, D., 2009. Cross-wind effects on road and rail vehicles. Veh. Syst. Dyn. 47 (8), 983–1022.

Beagles, A.E., Fletcher, D.I., 2013. The aerodynamic of freight: approaches to save fuel by optimizing the utilization of container trains. Proc. Inst. Mech. Eng. - Part F J. Rail Rapid Transit 14. May 2013.

CEN, 2010. EN14067-6. Railway Applications – Aerodynamics. - Part 6: Cross Wind. CEN, Brussels.

Cheli, F., Giappino, S., Rosa, L., Tomasini, G., Villani, M., 2013. Experimental study on the aerodynamic forces on railway vehicles in presence of turbulence. J. Wind Eng. Ind. Aerod. 123, 311–316.

Cheli, F., Di Gialleonardo, E., Melzi, S., Numerical analysis of the curving performance of low flatcar wagons. Int. J. Heavy Veh. Syst., vol. 18, p. 19–213.

Cui, T., Zhang, W., Sun, B., 2014. Investigation of train safety domain in cross wind in respect of attitude change. J. Wind Eng. Ind. Aerod. 130, 75–87.

Dorigatti, F., Sterling, M., Baker, C.J., Quinn, A.D., 2015. Crosswind effects on the stability of a model passenger train-A comparison of static and moving experiments. J. Wind Eng. Ind. Aerod. 138, 36–51.

European Rail Agency, 2008. Technical Specification for Interoperability (TSI 232/2008) – Rolling Stock Subsystem, 96/48/EC.

Giappino, S., Melzi, S., Tomasini, G., Villani, M., 2014. Experimental study on the effect of crosswind on a container train with different load configurations. In: Pombo, J. (Ed.), Proceedings of the Second International Conference on Railway Technology: Research, Development and Maintenance. Civil-Comp Press, Stirlingshire, UK. https://doi.org/10.4203/ccp.104.31. Paper 31.

Giappino, S., Rocchi, D., Schito, P., Tomasini, G., 2016. Cross wind and rollover risk on lightweight railway vehicles. J. Wind Eng. Ind. Aerod. 153, 106–112. https://doi.org/10.1016/j.jweia.2016.03.013. ISSN: 0167-6105.

Golovanevskiy, V.A., Chmovzh, V.V., Girka, Y.V., 2012. On the optimal model configuration for aerodynamic modeling of open cargo railway train. J. Wind Eng. Ind. Aerod. 107–108, 131–139.

Hemida, H., Baker, C., 2010. Large-eddy simulation of the flow around a freight wagon subjected to a crosswind. Comput. Fluids 39, 1944–1956.

Kedare, S.B., Sharma, S.C., Harsha, S.P., 2015. Computational fluid dynamics analysis of empty railway freight wagons. Int. J. Veh. Struct. Syst. 7 (1), 25–30.

Lai, Y.-C., Barkan, C.P., €Onal, H., 2008. Optimizing the aerodynamic efficiency of intermodal freight trains. Transl. Res. Part E Logist. Transp. Rev. 44 (5), 820–834.

Lai, Y.-C., Ouyang, Y., Barkan, C.P., 2008. A rolling horizon model to optimize aerodynamic efficiency of intermodal freight trains with uncertainty. Transport. Sci. 42 (4), 466–477.

Li, Y., Tian, H.-Q., 2012. Lateral aerodynamic performance and speed limits of doubledeck container vehicles with different structures. J. Cent. S. Univ. 19, 2061–2066.

Li, C., Burton, D., Kost, M., Sheridan, J., Thompson, M.C., 2017. Flow topology of a container train wagon subjected to varying local loading configurations. J. Wind Eng. Ind. Aerod. 169, 12–29.

Maleki, S., Burton, D., Thompson, M.C., 2017. Assessment of various turbulence models (ELES, SAS, URANS and RANS) for predicting the aerodynamics of freight train container wagons. J. Wind Eng. Ind. Aerod. 170, 68–80.

Niu, J.-Q., Zhou, D., Liang, X.-F., 2017. Experimental research on the aerodynamic characteristics of a high-speed train under different turbulence conditions. Exp. Therm. Fluid Sci. 80, 117–125.

Östh, J., Krajnović, S., 2014. A study of the aerodynamics of a generic container freight wagon using Large-Eddy Simulation. J. Fluid Struct. 44, 31–51.

Paradot, N., Grégoire, R., Stiepel, M., Blanco, A., Sima, M., Deeg, P., Schroeder-Bodenstein, K., Johnson, T., Zanetti, G., 2015. Crosswind sensitivity assessment of a representative Europe-wide range of conventional vehicles. Proc. Inst. Mech. Eng. Part F: J. Rail Rapid Transit 229 (6), 594–624.

Premoli, A., Rocchi, D., Schito, P., Tomasini, G., 2016. Comparison between steady and moving railway vehicles subjected to crosswind by CFD analysis. J. Wind Eng. Ind. Aerod. 156, 29–40.

Rail Accident Investigation Branch (RAIB), 1 March 2008. Detachment of Containers from Freight Wagons Near Cheddington and Hardendale.

Soper, D., Baker, C., Sterling, M., 2015. An experimental investigation to assess the influence of container loading configuration on the effects of a crosswind on a container freight train. J. Wind Eng. Ind. Aerod. 145, 304–317.

Zhang, J., Li, J.-j, Tian, H.-q, Gao, G.-j, Sheridan, J., 2016. Impact of ground and wheel boundary conditions on numerical simulation of the high-speed train aerodynamic performance. J. Fluid Struct. 61, 249–261.

Zhou, D., Tian, H.-Q., Yang, M.-Z., Lu, Z.-J., 2007. Comparison of aerodynamic performance of different kinds of wagons running on embankment of the Qinghai-Tibet Railway under strong cross-wind. Tiedao Xuebao/J. China Railw. Soc. 29 (5), 32–36.